Journal of Sound and Vibration 327 (2009) 249–253

Contents lists available at ScienceDirect

Journal of Sound and Vibration

journal homepage: www.elsevier.com/locate/jsvi

On the calculation of viscous damping of microbeam resonators in air

Claudio L.A. Berli [a,b,*], Alberto Cardona [c]

[a] INTEC (Universidad Nacional del Litoral-CONICET), Güemes 3450, 3000, Santa Fe, Argentina
[b] Dpto. Físico Matemática, FICH, UNL, Ciudad Universitaria, 3000, Santa Fe, Argentina
[c] CIMEC, INTEC (UNL-CONICET), Güemes 3450, 3000, Santa Fe, Argentina

ARTICLE INFO

Article history:
Received 24 January 2009
Received in revised form
28 May 2009
Accepted 2 June 2009
Handling Editor: C.L. Morfey
Available online 26 June 2009

ABSTRACT

Theoretical aspects concerning the calculation of the air damping of microbeam resonators in the framework of continuum fluid mechanics are discussed. A closed relationship between Knudsen and Stokes numbers is derived, which indicates that the no-slip flow regime is attained in systems that operate at high Stokes numbers only, while systems that operate at low Stokes numbers invariably enter the slip flow regime. These observations are relevant to improve the modelling and simulation of microbeam resonators integrated to micro-electromechanical systems (MEMS). In addition, analytical expressions of the viscous damping coefficients for different flow regimes are discussed in relation to experimental data.

1. Introduction

The dynamics of a flexural beam is governed by Bernoulli–Euler equation [1]. For a beam placed in the x_1-direction of the coordinate system (Fig. 1), the deflection function ϕ obeys to

$$EI\frac{\partial^4\phi}{\partial x_1^4}+m\frac{\partial^2\phi}{\partial t^2}+C_S\frac{\partial\phi}{\partial t}=f, \tag{1}$$

where E is Young's modulus, I is the moment of inertia, m is the mass per unit length, and C_S is the structural damping coefficient of the beam, which accounts for internal energy losses. Also in Eq. (1), the external force may be written as $f=f_{\text{drive}}+f_{\text{fluid}}$, where each term represents, respectively, the driving force that excites the beam and the viscous force due to the surrounding fluid [2]. It is known that f_{fluid} has two components: one is in-phase with the velocity, $C_V\partial\phi/\partial t$, thus denominated viscous damping, and the other is in phase with the acceleration, $m_a\partial^2\phi/\partial t^2$, hence denominated added mass [2,3]. The viscous coefficient C_V directly affects the quality factor Q, while m_a produces a shift in the resonance frequency of the beam. Therefore, a proper evaluation of f_{fluid} is crucial to improve the accuracy of computation of the quality factor of microbeam resonators integrated to MEMS [4,5], as well as to optimize cantilevers used in atomic force microscopy [2,3,6], microconverters [7], and biosensors [8].

In the framework of continuum fluid mechanics, viscous forces are determined from the fluid stresses acting on the body surface [9]. For this purpose, the fluid velocity $\mathbf{u}(\mathbf{x})$ and pressure $p(\mathbf{x})$ fields around the vibrating beam are obtained by

* Corresponding author at: INTEC (Universidad Nacional del Litoral-CONICET), Güemes 3450, 3000, Santa Fe, Argentina. Tel.: +54 342 4559174/75/76/77; fax: +54 342 4550944.
E-mail address: cberli@santafe-conicet.gov.ar (C.L.A. Berli).

0022-460X/$ - see front matter © 2009 Elsevier Ltd. All rights reserved.
doi:10.1016/j.jsv.2009.06.003

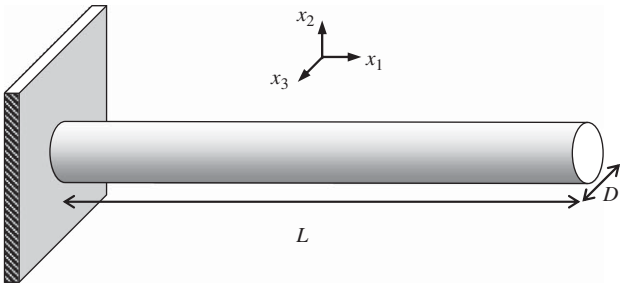

Fig. 1. Schematic representation of a cylindrical beam operating as a cantilever in a large gaseous environment.

solving Navier–Stokes (NS) equations,

$$\frac{\partial \mathbf{u}}{\partial t} + (\mathbf{u} \cdot \nabla)\mathbf{u} = -\frac{\nabla p}{\rho_f} + \nu \nabla^2 \mathbf{u}, \quad \nabla \cdot \mathbf{u} = 0, \tag{2}$$

where ρ_f is the fluid density and $\nu = \mu/\rho_f$ is the fluid kinematic viscosity, μ being the viscosity coefficient (the body force due to gravity is normally neglected in MEMS). Under harmonic motion conditions, the gas surrounding a resonating beam follows the oscillatory motion of the beam with angular frequency ω. Hence the scaling parameter for the fluid dynamic problem is the Stokes number,

$$\mathrm{St} = \omega D^2/4\nu, \tag{3}$$

which is defined as the ratio between inertial and viscous forces (D is a characteristic length for the particular flow, the cross-sectional width of the beam in this case; Fig. 1). This dimensionless number is also referred to as the kinetic Reynolds number in the literature [2,3,6,7]. In particular, if $\mathrm{St} \ll 1$, inertial effects may be neglected in Eq. (2), which leads to the Stokes model, a formulation normally preferred for the sake of simplicity. Nevertheless, microbeams resonators involve very high frequencies. For this reason, St numbers are relatively large and the full NS equations are usually needed.

When the fluid is air or another gas, choosing the appropriate velocity values at the beam surface, u_{wall}, is a key step in modelling. In fact, gas flow presents different regimes due to rarefaction effects, which can be characterized by the Knudsen number,

$$\mathrm{Kn} = \lambda/D, \tag{4}$$

where λ is the mean free path of molecules (inversely proportional to the gas pressure). There is consensus in the literature [10–12] that gas microflows can be treated in the classical framework of continuum fluid mechanics if $\mathrm{Kn} < 0.001$, i.e. by using NS equations with the no-slip boundary condition,

$$u_{\mathrm{wall}} = U, \tag{5}$$

where U is the tangential velocity of the beam. In the range $0.001 < \mathrm{Kn} < 0.1$, NS equations are still valid, but slip boundary conditions must be applied, such as the classical Maxwell slip-velocity equation,

$$u_{\mathrm{wall}} = U + \lambda \left.\frac{\partial u}{\partial x}\right|_{\mathrm{wall}}, \tag{6}$$

here written for the case of fully diffuse reflection (a review on the main models of the slip boundary condition is given in [12]). In Eq. (6), x represents the direction locally normal to the wall. When $\mathrm{Kn} > 0.1$, the continuum fluid mechanics breaks down, and there is a transitional flow region towards the free molecule flow, where statistical approaches are required [11]. Let us note here that $\lambda = 65$ nm for ideal gases at standard conditions of temperature and pressure. This value indicates that the beam cross-sectional size at which continuum fluid mechanics breaks down is $D \sim 1$ μm at normal pressure. Therefore, the flow around micro-scale beams at normal pressure can be modelled by using Eq. (2) with either Eq. (5) or (6), but the flow around nano-scale beams needs a different treatment.

The aim of this work is to discuss the formulation of the fluid dynamics problem for the evaluation of air damping when $\mathrm{Kn} < 0.1$. More precisely, we observe that the type of boundary condition to be applied (slip/no-slip) is also linked to the Stokes number of the system, which defines the (steady/unsteady) character of the flow. In what follows we study the Stokes numbers inherently associated to microbeam resonators in air. It is worth to mention that we are dealing with microbeams immersed in a large gaseous environment, and placed far from the walls. Examples of application of microbeams in these conditions are vibrating beams accelerometers (Fig. 2), whose work principle is based on the frequency shift of a vibrating quartz microbeam [13,14]. Other specific flow problems appearing in MEMS, like squeeze film damping [15] are not considered in the present analysis.

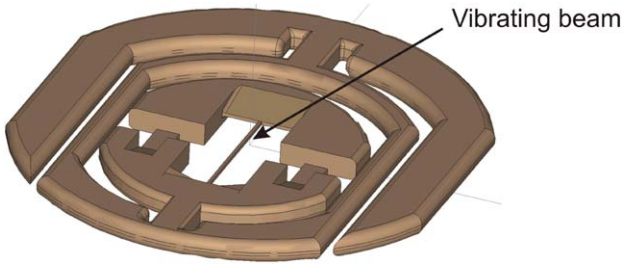

Fig. 2. Vibrating inertial accelerometer transducer [13,14].

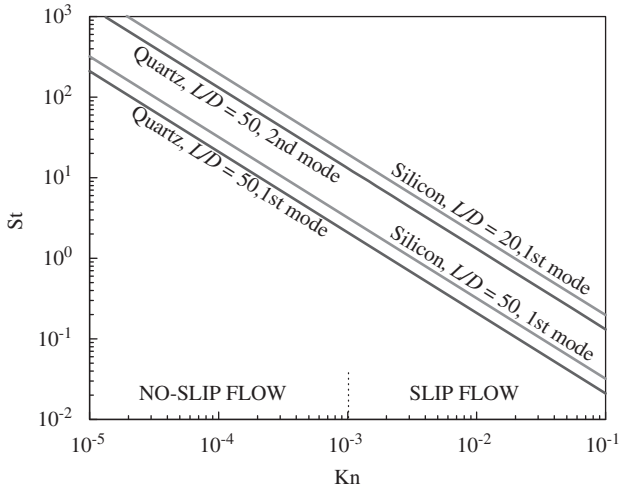

Fig. 3. Stokes number as a function of Kudsen number for cylindrical beam resonators in air. Lines represent the prediction of Eq. (7) with $\nu = 15 \times 10^{-6}\,\mathrm{m^2/s}$, $\lambda = 65\,\mathrm{nm}$, $E/\rho = 8290\,\mathrm{m/s}$ for silicon, and $E/\rho = 5440\,\mathrm{m/s}$ for quartz glass.

2. Flow regimes for the gas surrounding a vibrating beam

For a transversely vibrating beam of circular cross-section, with diameter D and length $L \gg D$ (Fig. 1), the resonance frequency for the i-th mode in vacuum is $\omega_i = \kappa_i^2 (E/16\rho)^{1/2} D/L^2$, where ρ is the density of the beam, and $\kappa_1 = 1.875$, $\kappa_2 = 4.694$, …, for a flexural beam operating as a cantilever [1–3]. As a first approximation, we may use ω_i to scale the beam resonance frequency in air. Thus the Stokes number (Eq. (3)) can be expressed in terms of the beam characteristics as follows, $\mathrm{St} = (\kappa_i/4)^2 (E/\rho)^{1/2} (D/L)^2 D/\nu$. It is observed that, for a fixed aspect ratio L/D, St varies linearly with D. Therefore, introducing the Kn number (Eq. (4)) yields the following relationship for the gas flow in the surroundings of a microbeam resonator:

$$\mathrm{St}\,\mathrm{Kn} = \left(\frac{\kappa_i}{4}\right)^2 \left(\frac{E}{\rho}\right)^{1/2} \left(\frac{D}{L}\right)^2 \frac{\lambda}{\nu}. \tag{7}$$

The right hand side of this expression accounts for the beam material (E/ρ), the beam aspect ratio (L/D), and gas properties (λ/ν). It is worth noting here that, for ideal gases in the continuum approximation, the ratio λ/ν does not depend on air pressure but on temperature [10–12]. Thus the product St Kn keeps constant when air pressure changes.

Following Eq. (7), Fig. 3 presents the Stokes numbers for cylindrical beams vibrating in air at room temperature, as a function of Knudsen numbers, in the region where the continuum approximation is valid ($\mathrm{Kn} < 0.1$). Different curves in Fig. 3 are aimed to illustrate the effect of beam material, aspect ratio and resonance mode. In any case, it is evident that the no-slip flow regime involves $\mathrm{St} > 1$, while the slip flow regime involves $\mathrm{St} \leq 1$. The analysis carried out here refers to cylindrical beams; however, the general findings can be extrapolated to cantilevers of rectangular cross-section [2,6].

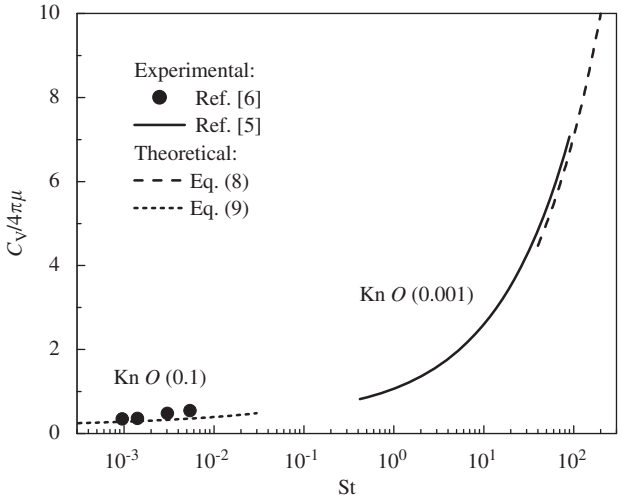

Fig. 4. Viscous coefficient as a function of Stokes number for different flow regimes.

3. Viscous damping in different flow regimes

Fig. 3 offers relevant information to be taken into account in modelling the air damping of microbeam resonators by using continuum fluid mechanics (Kn$<$0.1), i.e. to calculate $\mathbf{u}(\mathbf{x})$, $p(\mathbf{x})$, and then C_V and Q:

(i) Systems that operate at high Stokes numbers involve the no-slip flow regime. Consequently, analytical/numerical models should be based on the full NS equations (2) and boundary condition (5). Analytical expressions of the damping coefficients for cylinders under these conditions are available [16] . In particular, for St$\gg$1, their result simplifies to,

$$C_V = 4\pi\mu\left(\frac{\mathrm{St}}{2}\right)^{1/2}. \tag{8}$$

The analysis has been reworked lately for microbeam resonators [2,3], then confirmed by experiments [17] and numerical calculations [18]. The modelling of cantilever dynamics in this regime has been systematically improved [19].

(ii) Systems that operate at low Stokes numbers invariably enter the slip flow regime. Consequently, analytical/numerical formulations should account for the slip velocity at the beam surface. An analytical expression of the damping coefficient for cylinders at St$\ll$1 has been reported [20], which is based on Stokes equations and the slip boundary condition (6); that is,

$$C_V = \frac{4\pi\mu}{\log(4/\mathrm{St}^*) - \gamma + 1/2 + c\mathrm{Kn}}, \tag{9}$$

where $\mathrm{St}^* = DU/2\nu$, $\gamma = 0.5572$ is Euler's constant and $c \approx 1.8$ is a coefficient. It is appropriate to mention that beam resonators in the slip regime are usually modelled as a string of oscillating spheres (for instance, [8]). For the purposes of illustration, Fig. 4 compares the prediction of Eq. (9) with experimental data reported in the literature [6], corresponding to four nanobeam resonators in air, for which Kn is on the order of 0.1.

(iii) In the intermediate region, say Stokes numbers between 0.1 and 10, the full problem must be formulated, which necessarily require numerical calculations. Abundant experimental data found in the literature fall in this region. As an example, the full line in Fig. 4 condenses results obtained from silicon microbeams in air [5], for which Kn is on the order of 0.001.

4. Concluding remarks

Eq. (7) reveals that the scaling parameters St and Kn that characterize the gas flow in the surroundings of microbeam resonators are closely related. Accordingly, Fig. 3 shows the flow regimes that can be reached by microbeams in air. It is relevant to note that attaining a regime with St$<$1 and Kn$<$0.001 is virtually impossible in practice. Therefore, analytical/numerical models of fluid damping that include the no-slip boundary condition should not be extrapolated

straightforwardly to the case of gaseous environment at low St. This aspect is important to note because it is frequently misunderstood in the literature (see, for example, [4–6]). In the slip regime, the viscous damping appears to depend on Kn as well, as indicated by Eq. (9). Finally one may conclude that recognizing the gas flow regimes associated to microbeam resonators is relevant to properly model, and hence compute, air damping effects.

Acknowledgments

The authors wish to thank Agencia Nacional de Promoción Científica y Tecnológica (PAE 22592) and Consejo Nacional de Investigaciones Científicas y Técnicas, Argentina, for the financial aid received.

References

[1] S.M. Han, H. Benaroya, T. Wei, Dynamics of transversely vibrating beams using four engineering theories, *Journal of Sound and Vibration* 225 (1999) 935–988.
[2] J.E. Sader, Frequency response of cantilever beams immersed in viscous fluids with applications to the atomic force microscope, *Journal of Applied Physics* 84 (1998) 64–72.
[3] S. Kirstein, M. Mertesdorf, M. Schönhoff, The influence of viscous fluid on the vibration dynamics of scanning near-field optical microscopy fiber probes and atomic force microscopy cantilevers, *Journal of Applied Physics* 84 (1998) 1782–1790.
[4] C. Zhang, C. Xu, J. Qu, Analysis of the air-damping effect on a micromachined beam resonator, *Mathematics and Mechanics of Solids* 8 (2003) 315–321.
[5] W. Zhang, K. Turner, Frequency dependent fluid damping of micro/nano flexural resonators: Experiment, model and analysis, *Sensors and Actuators A* 134 (2007) 594–599.
[6] K. Yum, Z. Wang, A.P. Suryavanshi, M.-F. Yu, Experimental measurement and model analysis of damping effect in nanoscale mechanical beam resonator in air, *Journal of Applied Physics* 96 (2004) 3933–3938.
[7] H. Nouira, E. Foltête, L. Hirsinger, S. Ballandras, Investigation of the effects of air on the dynamic behavior of a small cantilever beam, *Journal of Sound and Vibration* 305 (2007) 243–260.
[8] V. Cimalla, F. Niebelschütz, K. Tonisch, Ch. Foerster, K. Brueckner, I. Cimalla, T. Friedrich, J. Pezoldt, R. Stephan, M. Hein, O. Ambacher, Nanoelectromechanical devices for sensing applications, *Sensors and Actuators B* 126 (2007) 24–34.
[9] F.M. White, *Viscous Fluid Flow*, MacGraw-Hill, New York, 1975.
[10] M. Gad-el-Hak, The fluid mechanics of microdevices—the Freeman Scholar Lecture, *Journal of Fluid Engineering* 121 (1999) 5–33.
[11] R.B. Bhiladvala, Z.J. Wang, Effects of fluids on the *Q* factor and resonance frequency of oscillating micrometer and nanometer scale beams, *Physical Review E* 69 (2004) 036307-1–036307-5.
[12] S. Colin, Rarefaction and compressibility effects on steady and transient gas flows in microchannles, *Microfluidics and Nanofluidics* 1 (2005) 268–279.
[13] O. Le Traon, D. Jamiaud, S. Muller, Monolithic accelerometer transducer, US Patent No. 5962786, 1999.
[14] S. Masson, O. Le Traon, D. Janiaud, Finite element analysis using OOFELIE: piezo-thermo-elastic simulations for vibrating inertial sensors, *Proceedings of the 10th Samtech Users Conference,* Liège, Belgium, 2007.
[15] V. Ostacevicius, R. Dauksevicius, R. Gaidys, A. Palevicius, Numerical analysis of fluid–structure interaction effects on vibrations of cantilever microstructure, *Journal of Sound and Vibration* 308 (2007) 660–673.
[16] S.S. Chen, M.W. Wambsganss, J.A. Jendrzejczyk, Added mass and damping of a vibrating rod in confined viscous fluid, *Transactions of ASME Journal of Applied Mechanics* 43 (1976) 325–329.
[17] J.W.M. Chon, P. Mulvaney, J.E. Sader, Experimental validation of theoretical models for the frequency response of atomic force microscope cantilever beams immersed in fluids, *Journal of Applied Physics* 87 (2000) 3978–3988.
[18] A. Maali, C. Hurth, R. Boisgard, C. Jai, T. Cohen-Bouhacina, J.-P. Aimé, Hydrodynamics of oscillating atomic force microscopy cantilevers in viscous fluids, *Journal of Applied Physics* 97 (2005) 074907-1–074907-6.
[19] C.A. Van Eysden, J.E. Sader, Frequency response of cantilever beams immersed in viscous fluids with applications to the atomic force microscope: arbitrary mode order, *Journal of Applied Physics* 101 (2007) 044908-1–044908-11.
[20] K. Tamada, Y. Inoue, Slip flow past an elliptic cylinder, *Japan Society for Aeronautical and Space sciences, Transactions* 19 (1976) 140–148.